Chapter 3. Characterization techniques and reaction analysis

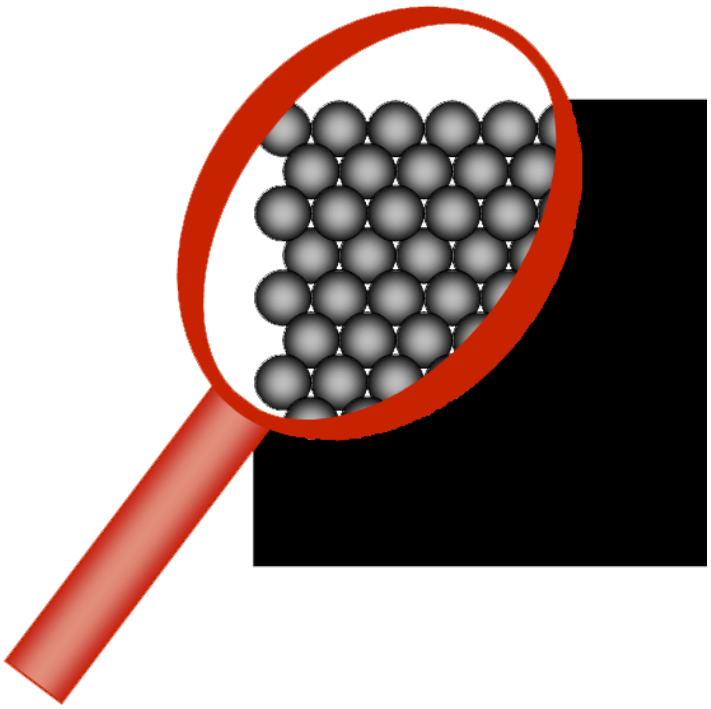

This chapter:

(i) Succinctly explains the underlying principles of the characterization techniques, employed in our works, with emphasis on how we exploited these techniques and which information we acquired regarding the physical and chemical properties of the prepared materials.

(ii) Describes calculation of the reaction efficiencies and quantitative analysis of the fatty acids with GC-MS.

3.1 Characterization techniques

3.1.1 X-ray Diffractometry

X-ray diffraction (XRD) is among the most powerful techniques for the characterization of solids. It is used to identify crystalline phases by means of lattice structural parameters, and to obtain an indication of crystallite size. X-ray diffraction occurs in the elastic scattering of X-ray photons by atoms in a periodic lattice. The scattered monochromatic X-rays that are in phase give constructive interference. According to Bragg's law, the constructive interference occurs only when the path length difference between two or more beams diffracted in the same direction is an integer multiple of the wavelength (Figure 3.1). The path length difference is dependent on the lattice spacing of the atoms and the sine function of the angle between the incident angle and the scattering angle.

$$n\lambda = 2d\sin\theta \tag{3.1}$$

where λ is the wavelength of the X-rays, d is the distance between two lattice planes, θ is the angle between the incoming X-rays and the normal to the reflecting lattice plane, n is an integer called the order of the reflection.

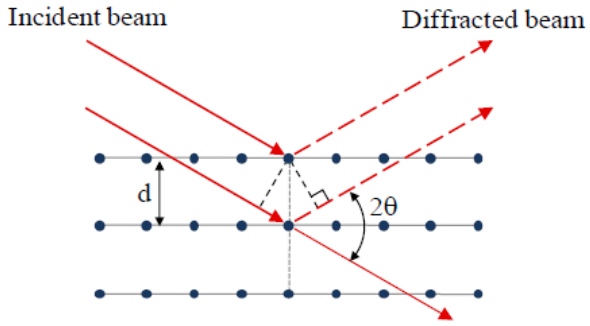

Figure 3.1. Schematic illustration of the Bragg's law.

A typical XRD instrument consists of three main parts: X-ray tube, specimen stage, and X-ray detector. The X-ray beam generated by the X-ray tube passes through special slits, which collimate the X-ray beam and prevent beam divergence. After passing through the slits, the X-ray

beam strikes the specimen that is supported by the plane of specimen. The X-rays diffracted by the specimen interfere constructively when they are in phase and produce a convergent beam at receiving slits before entering the detector. By continuously changing the incident angle of the X-ray beam, diffraction intensity is recorded in a range of 2θ.

In our study, XRD was used to identify the crystalline phases of various structures of tungsten and molybdenum oxides. We have worked with X'Pert HighScore Software to analyze the XRD data. The obtained spectra were compared with the updated database of ICDD[3] library of spectra. In principle, if the angles, 2θ, under which constructively interfering X-rays leave the crystal, can be measured, the Bragg relation gives the corresponding lattice spacings, which can be used to identify the crystalline phase of the sample.

3.1.2 Infrared Spectroscopy

Infrared spectroscopy (IR) studies the changes in the vibrational and rotation movements of the molecules. It is commonly used to show the presence or absence of functional groups which have specific vibration frequencies. In our research, since XRD technique revealed bulk chemical structure of the obtained samples, FTIR analysis was employed to learn more about the composition of organic part of the hybrid organic-inorganic samples as well as different available tungsten and molybdenum bonds in crystalline structures of the samples.

In principle, at ordinary temperatures, organic molecules are in a constant state of vibrations, each bond having its characteristic stretching and bending frequencies. When infrared light radiations with frequency between 4000-400 cm^{-1} are passed through a sample of an organic compound, some of these radiations are absorbed by the sample and are converted into energy of molecular vibrations. The other radiations which do not interact with the sample are transmitted through the sample without being absorbed. The infrared spectrum of the sample or compounds is the plot of % transmittance against frequency. The presence of characteristic vibrational bands in an IR spectrum indicates the presence of the corresponding bonds in the sample under investigation.

[3] The International Center for Diffraction Data

3.1.3 Thermogravimetric analysis

Thermogravimetric analysis (TGA) is a technique in which the mass of a substance is monitored as a function of temperature or time while the temperature of the sample, in a specified atmosphere, is programmed. TGA is a very useful technique for analysis of thermal decomposition, oxidization, dehydration, heat resistance, and kinetics analysis. By combining with other measurement techniques, variety of information on one sample can be achieved. Simultaneous thermogravimetry and differential thermal analysis (TGA/DTA) is a method in which thermogravimetry and differential thermal analysis are combined and measured simultaneously by a single apparatus. In our works, TGA/DTA was efficiently used to not only determine the amount of surfactant molecules adsorbed on the surface of metal oxide catalysts, but also provide information related to certain physical and chemical phenomena that occur during heating.

In DTA, the temperature difference between the sample and a reference material is monitored against time or temperature while the sample's temperature, in a specified atmosphere, is programmed. Figure 3.2, which shows the measurement principles of DTA, elucidates its role in our works. It shows the temperature change of the furnace, the reference and the sample against time (Figure 3.2 a), and the change in temperature difference (ΔT) against time detected with the differential thermocouple. ΔT signal is referred to as the DTA signal. Materials that do not change in the measurement temperature range (usually α-alumina) are used as reference. When the furnace is heating, the reference and the sample begin to be heated with a slight delay depending on their respective heat capacity, and eventually heat up according to the furnace temperature. Therefore, ΔT changes until a static state is reached, and after achieving stability, reaches a set amount compliant with the difference in heat capacity between the sample and the reference. The signal at the static state is known as the baseline. Since then, by increasing the furnace temperature some either endothermic or exothermic phenomena might occur, which result in sudden decrease or increase in ΔT. For example, if melting occurs (as an endothermic process), the rise in the sample's temperature stops as shown in Figure 3.2 a, and the absolute value of ΔT increases. When the melting ends, the temperature curve rapidly reverts to the baseline. At this point, the ΔT signal reaches the peak, as shown in Figure 3.2 b. From this, we can detect the sample's transition temperature and the reaction temperature from the ΔT signal (DTA signal). In Figure 3.2 b, the

temperature difference due to the sample's endothermic change is shown as a negative direction and the temperature difference due to the sample's exothermic change is shown as a positive direction.

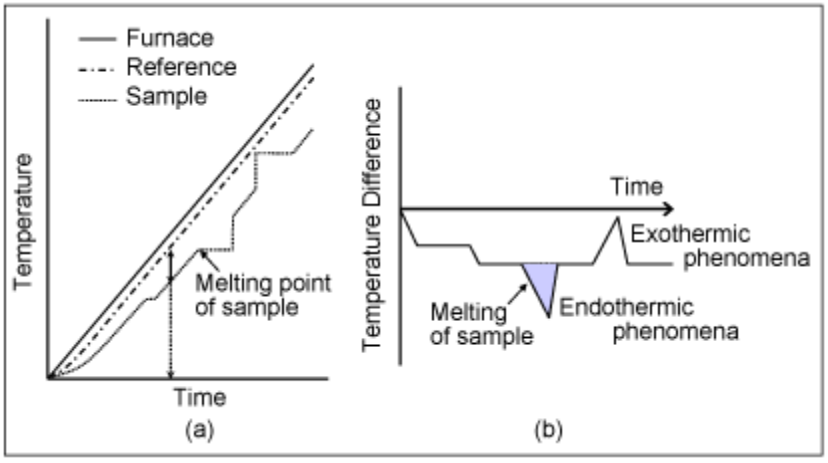

Figure 3.2. Measurement principles of DTA.

3.1.4 Nitrogen physisorption

Nitrogen physisorption is a widely used method for the characterization of porous materials with regard to the determination of surface area, pore size, pore size distribution, and porosity. This technique is based on the measurement of adsorption and desorption equilibrium isotherms of nitrogen on a solid surface at different partial pressures of nitrogen. The resulting relationship of volume of nitrogen adsorbed and desorbed *vs.* relative pressure at constant temperature is known as sorption isotherms. The shape of the isotherms strongly depends on the porous structure of the materials.

In 1985, the International Union of Pure and Applied Chemistry (IUPAC) published a classification of six types of sorption isotherms (Figure 3.3). Type I isotherms are characteristic of microporous materials. Type II and III isotherms are the normal form of adsorption by nonporous or macroporous adsorbents in which the adsorption proceeds via multilayer formation. Type IV and V isotherms are characteristic of multilayer adsorption consisting of capillary condensation onto mesoporous materials. Type VI isotherms represent stepwise multilayer adsorption on a uniform nonporous surface.

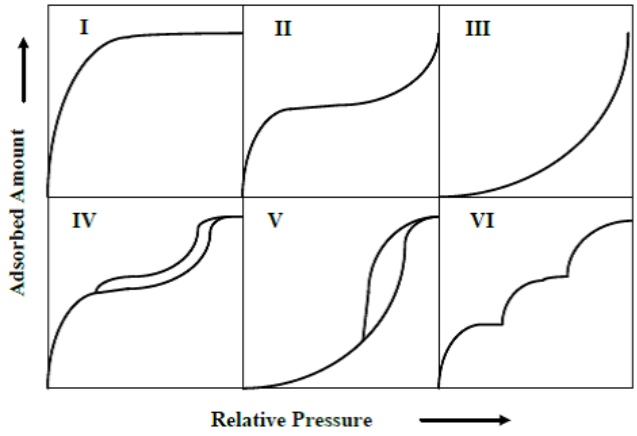

Figure 3.3. IUPAC classification of the physisorption isotherms.

To date, various theories are introduced to determine the surface area of porous materials. The Brunauer-Emmett-Teller (BET) method is the most widely used one. The BET equation is as follows:

$$\frac{P/P_0}{n(1-P/P_0)} = \frac{1}{n_m c} + \frac{c-1}{n_m c} \times \frac{P}{P_0} \qquad (3.2)$$

Where n is the number of moles adsorbed at the relative pressure P/Po, n_m is the monolayer capacity, c is a constant related exponentially to the heat of adsorption in the first adsorbed layer. A linear relationship between $\frac{P/P_0}{n\,(1-P/P_0)}$ and P/P_0 is obtained by the BET equation. The intercept $\frac{1}{n_m c}$ and slope $\frac{c-1}{n_m c}$ can be used to calculate the values of n_m and c. Therefore, the surface area can be computed from the monolayer capacity on the assumption of close packing:

$$A = n_m \alpha_m L \qquad (3.3)$$

Where α_m is the molecular cross-sectional area of the adsorbate, n_m is the monolayer capacity, and L is the Avogadro constant. Nitrogen is the most appropriate gas for surface area determination. If it is assumed that the BET monolayer is close-packed, then α_m will be 0.162 nm^2 at 77 K.

The pore-size distribution is usually determined by the BJH model (named after its discoverers Barrett, Joyner and Halenda) or non-local density functional NLDFT theory. The DFT methods were developed by taking into account the particular characteristics of the hysteresis like pore shape. Non-intersecting pores of different size are assumed to be of the same regular shape (cylinders, slits or spheres). Correspondingly, pore size distributions are calculated for a given pore geometry, using a series of theoretical isotherms (kernels) for pores of a given chemical composition of the respective geometry with different diameters. In principle, NLDFT method may be applied over the complete range of nanopore sizes when suitable kernels are available.

3.1.5 Electron microscopy

Electron microscopy has emerged as an extremely powerful tool to characterize micro and nanoscale materials. This technique can provide information about not only the size and shape of materials, but also their crystallographic structures and elemental compositions. In principle, electron microscopes use a beam of highly energetic electrons to examine objects on a very fine scale. The power and versatility of electron microscopy derives from the variety of ways in which the primary electron beam interacts with the sample, and the fact that the strength of the various interactions is very dependent on the sample's physical structure, topography, crystallography and chemistry. There are generally two types of electron microscope: transmission electron microscope (TEM) and scanning electron microscope (SEM). They exploit different signals generated from electron beam-atom interactions for material characterization. In the present research, electron microscopy was used to reveal the morphology, size, and shape of the samples. Moreover, SEM instrument provided some information on chemical composition of the samples via X-ray energy dispersive spectrometer (EDS).

3.1.6 Elemental analysis

The most reliable elemental analysis method to determine the contents of light elements like H, C, and N in a compound, to my knowledge, is Carbon/Hydrogen/Nitrogen/Sulphur (C/H/N/S) analysis, which is performed via the quantitative '*dynamic flash combustion*' method.

This technique is based on the complete and instantaneous oxidation of the sample. In our works, we have used this analysis to verify the structure of and propose a chemical formula for the prepared polyoxotungstates. The used instrument was EA 1108 Fisons, and the method of analysis is briefly explained here:

1. Approximatively 2 mg of sample are weighed in a tin container, which is placed inside an autosampler drum purged with a continuous flow of helium. The samples are introduced at preset intervals into a combustion reactor (quartz tube maintained at 1021 °C).
2. Inside this furnace, the helium stream is temporarily enriched with pure oxygen when the samples are dropped. The sample and its container melt. The tin promotes a violent reaction under these conditions, which leads to a complete oxidation of all the substances (even the thermally resistant ones). Quantitative conversion in combustion products (CO_2, H_2O, N_2, SO_2) is achieved by passing the mixtures of gases over the different layers of the reactor.
3. The combustion gases are separated by gas chromatography using helium as carrier gas. The detection is done using a thermal conductivity detector (TCD) giving an output signal proportional with the concentration of the components: C, H, N, S.
4. The calibration of the instrument is performed using certified standards and 'quality control' samples are run for validation of the results (see detailed procedure below).

A calibration curve is built using standards. Standards are also analysed as unknown for quality control purpose. The analyses are performed as follows:

3-6 analyses of standards (calibration curve)
1 analysis of a standard as unknown ('quality control' sample)
6-10 analyses (unknown)
1 analysis of a standard as unknown ('quality control' sample)
6-10 analyses (unknown)
3-6 analyses of standards (calibration curve)
1 analysis of a standard as unknown ('quality control' sample)

6-10 analyses (unknown)

1 analysis of a standard as unknown (‘quality control’ sample)

6-10 analyses (unknown)

3-6 analyses of standards (calibration curve)

……

Certified standards from the company Isomass are used. The standards having % C, N, H, S close to those of the unknown samples are chosen. For the ‘quality control’ samples the validation criteria versus the expected values for the standards used are presented in Table 3.1.

Table 3.1. Concordance criteria of CHNS analysis [1].

% of each element	Accepted difference
C, H, N	
5.00 – 9.99	± 0.15
10.0 – 24.9	± 0.25
25.0 – 90.0	± 0.30
S	
< 25.0 [1]	± 1.00

1. For the samples containing more than 25 % S, the instrument is less reliable.

Duplicate analyses are always performed for each unknown sample. The strict concordance criteria for the two analyses of the same sample are presented in Table 3.1 (differences of ± 0.30 % for C, H, N, and ± 1.00 % for S are usually considered acceptable). The results not being concordant could indicate: presence or impurities, heterogeneity, decomposition, other. The detection limits for the analyses are the following: 0.3 % for C, H, N and 1.0 % for S.

3.1.7 Zeta potential analysis

Zeta potential analysis is critical in understanding the electrical charge characteristics of sample particles. The electrical charge properties control the interactions between particles and therefore determine the overall behavior of a sample suspension.

The liquid layer surrounding the particle exists as two parts; an inner region (Stern layer) where the ions are strongly bound and an outer (diffuse) region where they are less firmly associated. Within the diffuse layer, there is a notional boundary inside which the ions and particles

form a stable entity. When a particle moves (*e.g.*, due to gravity), ions within the boundary move with it. Those ions beyond the boundary stay with the bulk dispersant. The potential at this boundary (surface of hydrodynamic shear) is the zeta potential (Figure 3.4).

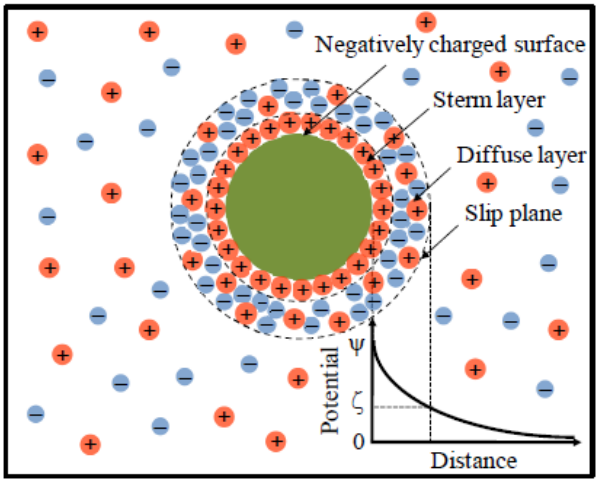

Figure 3.4. Zeta potential and ionic distribution of a negatively charged particle.

The zeta potential of a particle cannot be measured directly, but can be calculated from measurements of the velocity of a particle in suspension when an electric field is applied. Particle velocity in the liquid, referred to as electrophoretic velocity, depends on the strength of the electric field, the dielectric constant of the liquid, the viscosity of the liquid, and the size and zeta potential of the particle. The electrophoretic velocity can be measured by using techniques called laser doppler velocimetry and phase analysis light scattering. The frequency shift or phase shift of an incident laser beam scattered by the sample particles moving in an electric field is measured and used to calculate the electrophoretic mobility.

The magnitude of the zeta potential gives an indication of the potential stability of the colloidal system. If all the particles in suspension have a large negative or positive zeta potential, then they will tend to repel each other and there will be no tendency for the particles to come together. However, if the particles have low zeta potential values then there will be no force to prevent the particles coming together and flocculating. In our study, zeta potential analysis was used to characterize the stability of the catalyst colloidal suspension.

3.2 Quantitative analysis of the catalytic tests

The most common method for the determination of the fatty acids composition in a lipid mixture is gas-liquid chromatography (GLC). In the terms of fatty acids reactions, since several substrates are usually involved in a reaction, it would be more beneficial to utilize a gas chromatograph equipped with a mass detector. In this way, the Gas chromatography-mass spectrometry (GC-MS) not only quantifies but also identifies the different chemicals in the reaction. Figure 3.5 shows a typical GC-MS system. Therefore, in our works, GC-MS analysis was used for the separation, identification, and quantification of the products after the reaction.

Due to the long chain and, also, presence of carboxyl functional group, fatty acids are highly polar compounds that tend to form hydrogen bonds. This affinity results in adsorption issues of fatty acids on the stationary phase inside of the GC capillary column. Therefore, fatty acids in their free form are difficult and fallible to analyze with GC. Although some polar stationary phases (such as FFAP column from Agilent Company) have been recently developed for direct analysis of free fatty acids, more accurate and reproducible chromatographic data are obtained if the fatty acids are derivatized to their respective methyl esters. Reducing the polarity of fatty acids make them more amenable for analysis. Converting fatty acids to fatty acid methyl esters is the most common method for preparation of fatty acids prior to GC analysis, because methyl esters offer excellent stability, and provide quick and quantitative samples for analysis. Moreover, neutralizing the polar carboxyl group leads to easier distinguish between the very slight differences exhibited by unsaturated fatty acids. Fatty acid methyl esters (FAMEs), then, can be separated by boiling point difference, degree of unsaturation, position of unsaturation, and even the *cis* and *trans* configurations of unsaturation.

3.2.1 Derivatization process prior to GC-MS analysis

Throughout our catalytic tests, after a typical oxidative cleavage reaction, the products mixture underwent a derivatization reaction, in which the expectedly produced azelaic and pelargonic acids, and possibly unreacted oleic acid were esterified to dimethyl azelate, methyl pelargonate, and methyl oleate, respectively. A general esterification reaction of fatty acids is shown in Equation 3.4. The process involves heating the acid in an alcoholic solvent (commonly

methanol) in the presence of an acidic catalyst. The role of catalyst in this reaction is protonation of oxygen in the carboxyl group (see Scheme 3.1, step 1) to make the acid more reactive to nucleophiles. Methanol molecule then reacts with the protonated acid (step 2) resulting in the loss of water and production of ester (step 3). This reaction is reversible, therefore to obtain a higher yield, removing water is necessary which can be done by using a water scavenger (such as anhydrous sulfuric acid and graphite bisulfate) or performing the reaction at temperatures higher than 100°C.

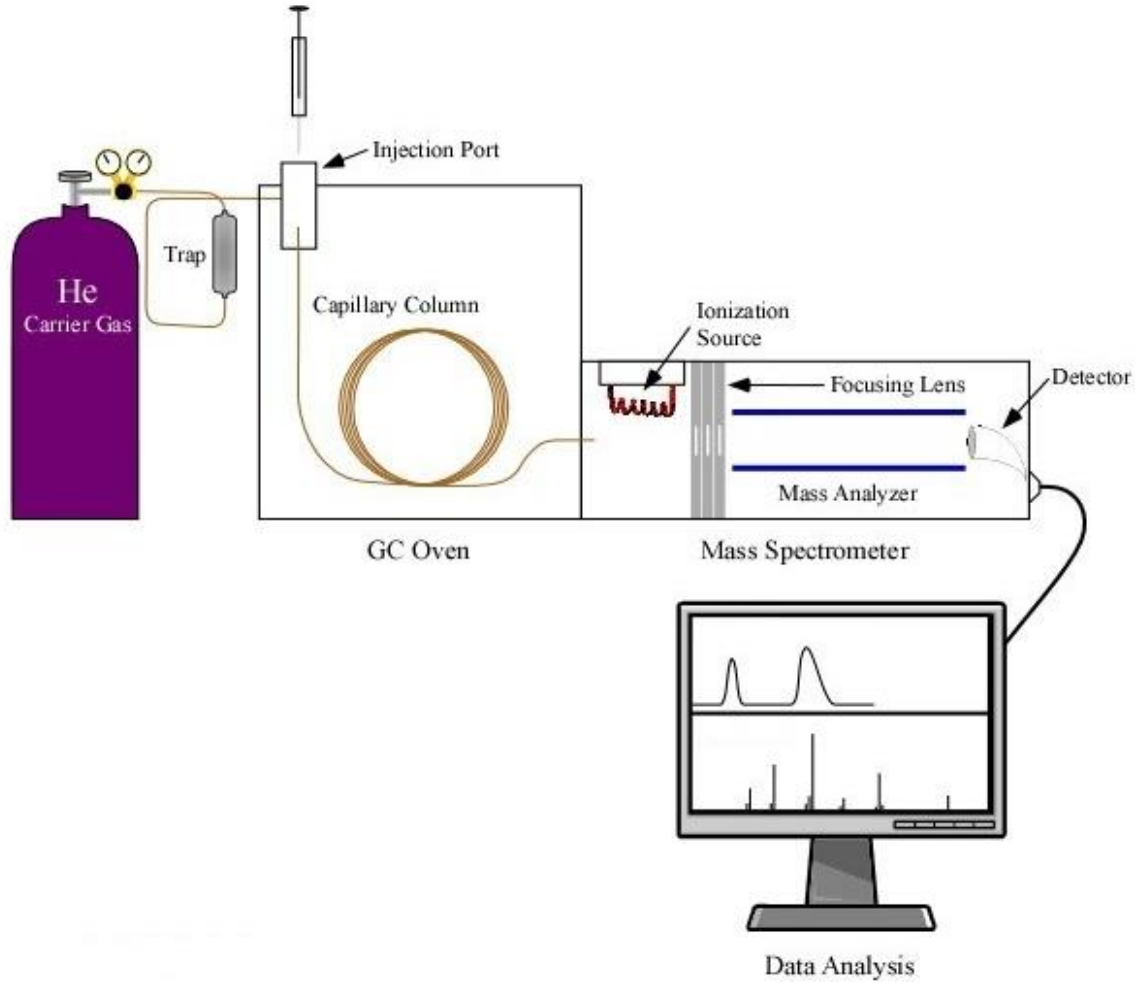

Figure 3.5. Different parts of a GC-MS system.

$$R\text{-}COOH + CH_3OH \rightarrow R\text{-}COO\text{-}CH_3 + H_2O \quad (3.4)$$

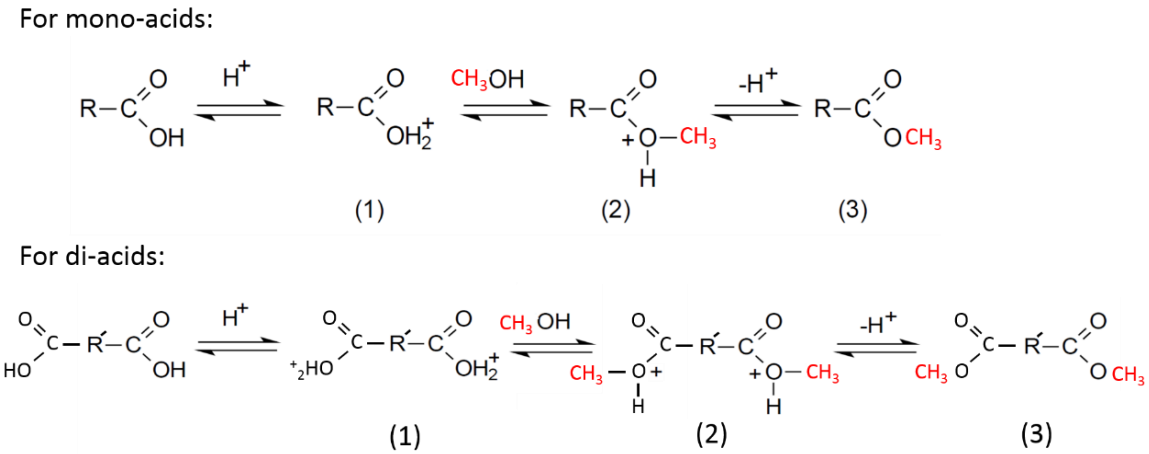

Scheme 3.1. Three steps mechanisms of esterification of mono and dicarboxylic acids over acid catalysts.

3.2.2 Chromatograms analysis and calculation procedure

First, the GC-MS was calibrated by the analytical standards of dimethyl azelate, methyl pelargonate, and methyl oleate. Obtaining the calibration curves is a very critical step in the quantitative analysis. In addition to the instrument's operating conditions, concentrations of the standard samples must be carefully chosen to obtain a linear calibration curve. A rule of thumb says not more than 500 ppm of analyte should enter to the mass detector to obtain a linear calibration curve. According to this and based on the flow rate of the carrier gas and the split ratio (see section 3.2.3), we calculated the proper concentration of the sample solutions for injection to GC-MS, which resulted in excellent linearity of the calibration curves. Admittedly, the calibration curves must be reproduced regularly. Figure 3.6 shows typical calibration curves obtained for methyl oleate, dimethyl azelate, and methyl pelargonate.

After the catalytic reaction (oxidative cleavage of oleic acid) and the derivatization process, a typical esterified sample, expectedly including dimethyl azelate, methyl pelargonate, and possibly methyl oleate, was injected to GC-MS. A constant and exact amount was injected each time, and the injection was repeated at least four times for each sample to be averaged. The peaks in the obtained chromatograms always had excellent shape and sharpness, owing to the carefully chosen column type and operating conditions of GC (see section 3.2.3), which lead to reliable results. Figure 3.7 shows a typical chromatogram of the reaction products. Based on peak areas in

the chromatograms and the calibration curves, conversion and yields of the oxidative cleavage reaction were calculated, using the following formulas:

$$Conversion = \frac{Total\ amount\ of\ oleic\ acid\ consumed\ (mole)}{Initial\ amount\ of\ oleic\ acid\ (mole)} \times 100 \qquad (3.5)$$

$$Yield_{(A)} = \frac{Amount\ of\ chemical\ A\ produced\ (mole)}{Total\ amount\ of\ oleic\ acid\ consumed\ (mole)} \times 100 \qquad (3.6)$$

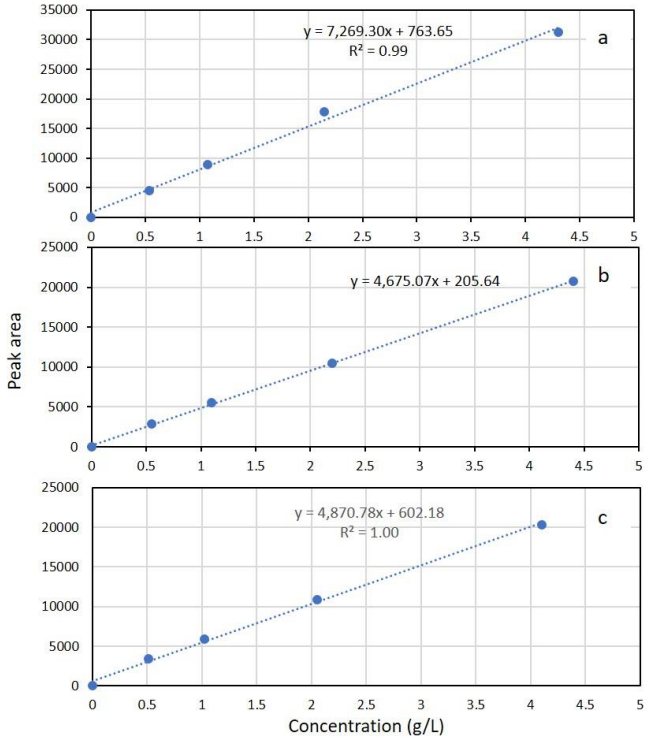

Figure 3.6. Typical calibration curves of (a) methyl oleate, (b) dimethyl azelate, and (c) methyl pelargonate.

The properly adjusted temperature programming allowed separation of methyl pelargonate, dimethyl azelate, and methyl oleate with discrete retention times (R_t) of 10.4, 15.8, and 26.8 min, respectively (see Figure 3.7). Some other peaks are also observed in the chromatograms, indicating presence of by-products, which were qualitatively analyzed by MS, as follows. Small and often negligible peaks in e.g. R_t= 6.8, 8.9, 11.2, and 16.7 min belonged to octanal, methyl esters of hexanoic and octanoic acids, and 9,10-dihydroxy octadecanoic acid, respectively, which were

produced by impurities of the reactants and/or insignificant side reactions (e.g. hydroxylation). Two relatively more considerable peaks in R_t= 8.6 and 13.8 min belonged to nonanal and 9-oxononanoic acid, respectively, which were produced by partial-oxidation of oleic acid. Since after minute 30 no significant peak was obtained, the chromatograms have been generally monitored up to R_t= 30 min.

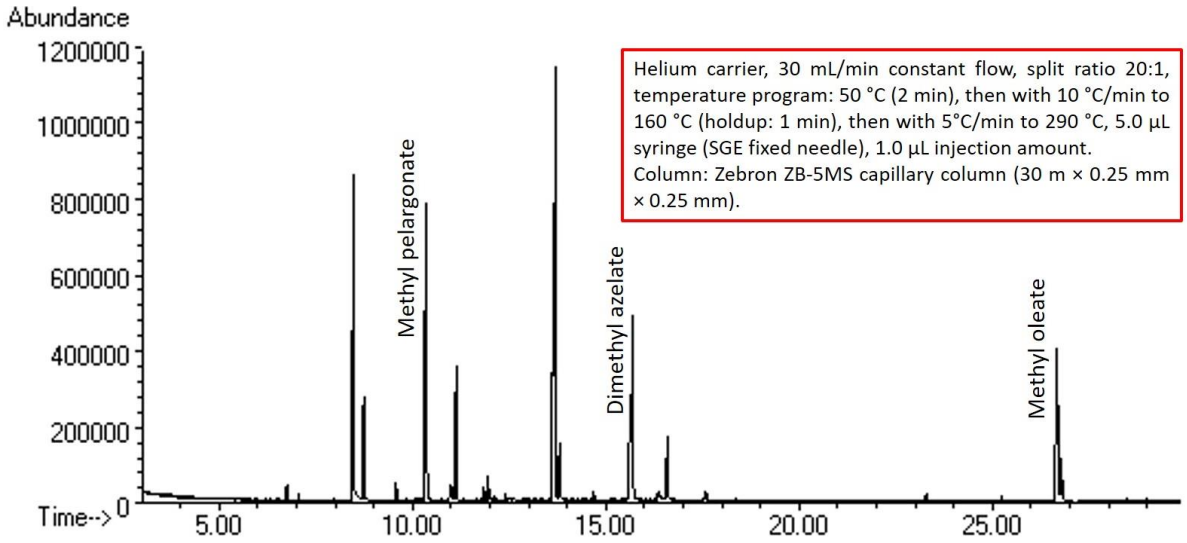

Figure 3.7. A typical gas chromatogram of the products (after derivatization) of oxidative cleavage of oleic acid.

It should be noted that such by-products like 9-oxononanoic acid, which are the direct result of involvement of carboxylic group in the reaction, has made oxidative cleavage of unsaturated fatty acids, compared to alkenes and cyclic olefins, more complicated and investigation of their reaction mechanism more difficult. It makes more sense given the fact that 9-oxononanoic acid is not commercially available (in known chemical provider companies), which makes calibration of chromatography systems by the analytical standard of this chemical, and consequently its quantitative analysis by these systems impossible.

3.2.3 Apparatus and design

The GC-MS included a Hewlett-Packard HP 5890 series GC system and MSD Hewlett-Packard model 5970. GC system was equipped with Zebron ZB-5MS capillary column (30 m × 0.25 mm × 0.25 mm). Helium was used as a carrier gas with the flow rate of 30 mL/min. A split

ratio of 20:1 was fixed. The front inlet temperature was 280 °C. The oven temperature program consisted of maintaining at 50 °C for 2 min, then a ramp rate of 10 °C/min to 160 °C following by a hold-up time of 1 min, and further increase with the rate of 5°C/min to 290 °C. Direct injection by a 5.0 µL syringe (SGE fixed needle, 23-26 gauge/42mm L/Cone Tip, Phenomenex Co.) was employed with 1.0 µL injection amount for each run. HP Chemstation software was used to analyze data.